

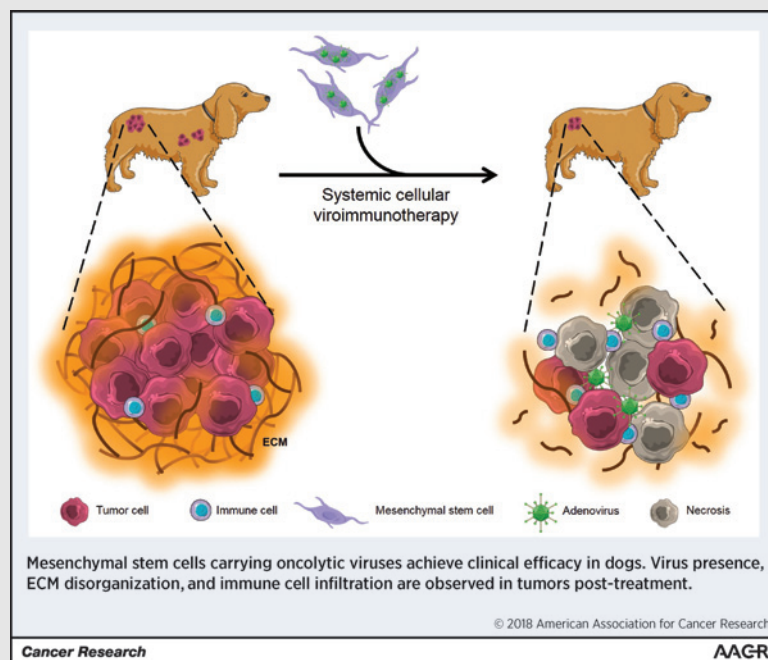
Remission of Spontaneous Canine Tumors after Systemic Cellular Viroimmunotherapy

Teresa Cejalvo¹, Ana Judith Perisé-Barrios¹, Isabel del Portillo², Eduardo Laborda³, Miguel A. Rodríguez-Milla¹, Isabel Cubillo¹, Fernando Vázquez², David Sardón², Manuel Ramírez⁴, Ramon Alemany³, Noemí del Castillo², and Javier García-Castro¹



Abstract

Dogs with spontaneous tumors treated in veterinary hospitals offer an excellent opportunity for studying immunotherapies, including oncolytic viruses. Oncolytic viruses have advanced into the clinic as an intratumorally administered therapeutic; however, intravenous delivery has been hindered by neutralization in the blood. To circumvent this hurdle, mesenchymal stem cells have been used as a "Trojan horse." Here, we present the treatment of 27 canine patients with cancer with canine mesenchymal stem cells infected with ICOCV17, a canine oncolytic adenovirus. No significant adverse effects were found. The response rate was 74%, with 14.8% showing complete responses, including total remissions of lung metastasis. We detected virus infection, stromal degeneration, and immune cell infiltration in tumor biopsies after 4 weeks of treatment. The increased presence of antiadenoviral antibodies in the peripheral blood of treated dogs did not appear to prevent the clinical benefit of this therapy. These data indicate that oncolytic viruses loaded in mesenchymal stem cells represent an effective cancer immunotherapy.



Significance: The classical clinical limitations of antitumoral viroimmunotherapy can be overcome by use of mesenchymal stem cells.

Graphical Abstract: <http://cancerres.aacrjournals.org/content/canres/78/17/4891/F1.large.jpg>. *Cancer Res*; 78(17); 4891–901. ©2018 AACR.

¹Unidad de Biotecnología Celular, ISCIII, Madrid, Spain. ²Veterinary Hospital, Alfonso X University, Madrid, Spain. ³Institut Català d'Oncologia, IDIBELL, Barcelona, Spain. ⁴Servicio de Oncohematología y Trasplante, Hospital Universitario Niño Jesús, Madrid, Spain.

Note: Supplementary data for this article are available at Cancer Research Online (<http://cancerres.aacrjournals.org/>).

T. Cejalvo and A.J. Perisé-Barrios contributed equally to this article.

Corresponding Author: Javier García-Castro, Avda. Majadahonda-Pozuelo Km 2, Madrid 28220, Spain. Phone: 34918223288; Fax: 34918223268; E-mail: jgcastro@isciii.es

doi: 10.1158/0008-5472.CAN-17-3754

©2018 American Association for Cancer Research.

Introduction

Oncolytic viruses have shown great potential as anticancer therapies with the recent FDA and European Medicines Agency approvals of Amgen's Imlygic as an intralesional treatment for patients with melanoma (1). However, systemic administration of oncolytic viruses would be preferred in many cases because solid tumors are not always accessible. In fact, oncolytic viruses can be intravenously delivered safely not only with limited toxicity, but also with limited efficacy (2). As a therapeutic alternative, the use of cells that function as a "Trojan horse" delivery vehicle has been proposed. Carrier cells are infected *in vitro* and injected systemically to home into tumor beds and release oncolytic viruses (3). We have developed this strategy for

pediatric solid tumors (4) using human mesenchymal stem cells (MSC) infected with ICOVIR-5, a human oncolytic adenovirus, which we have called Celyvir (5). We reported our initial human clinical results on the use of Celyvir in patients with advanced neuroblastoma where we described an excellent toxicity profile and several clinical responses, including two complete remissions out of 12 patients (6, 7). This supported an ongoing phase I clinical trial for pediatric and adult tumors (ClinicalTrials.gov Identifier: NCT01844661). In this study, we improve upon our antitumoral therapy as a method to treat spontaneously occurring tumors in canine patients. Clinical trials conducted in client-owned dogs are very useful for developing new anticancer therapeutics (8, 9) for human and veterinary medicine. Histologic and genetic molecular alterations that correlate with cancers in dogs and humans are analogous (10, 11), and surgery or oncology treatments for humans and dogs are nearly identical.

We sought to determine the safety and potential efficacy of systemic injections in dog patients of an upgraded canine version of Celyvir (dCelyvir), using dog MSCs (dMSC) and ICOCAV17, a new canine oncolytic adenovirus (12). Previously, we used this virus via intratumoral administration to treat six dogs with different tumor types inducing partial responses (PR) and stabilization disease (SD; ref. 12). Now, in addition to using MSCs as carriers, we have focused mainly on canine patients with sarcomas and central nervous system (CNS) tumors, because our primary objective is pediatric cancer and carcinomas are infrequent in childhood. Although some subtypes of human soft-tissue sarcoma (STS) are sensitive to chemotherapeutic agents, the outcome of chemotherapy is unsatisfactory rendering overall response rates of about 25% as a first-line treatment (13, 14). The potential for immunotherapy in the treatment of sarcomas is beginning to be explored (15), and oncolytic viruses have recently been used for sarcoma treatments with encouraging results (16, 17).

Here, in a veterinary trial with dCelyvir in 27 canine patients, we observed an excellent toxicity profile as well as a clinical benefit in 74% of patients, including 14.8% showing complete remissions. Our results also show microenvironment alterations and immune cell infiltration in tumors after dCelyvir treatment, suggesting the activation of antitumor immune responses. We believe that the immune-related response of MSCs when infected with oncolytic adenoviruses has an important role in observed clinical benefit.

Materials and Methods

Clinical study and canine patients

We enrolled 27 canine patients between March 2013 and March 2016, for treatment with dCelyvir. The clinical study was approved by the Veterinary Hospital Ethics Committee, and all patient owners gave written informed consent. Inclusion criteria were owner refusal or disease progression to standard treatment (chemotherapy/surgery), absence of severe undercurrent disease, and docile character for easy treatment without sedation. The study included different dog breeds. The diagnosis was performed analyzing tumor biopsies. In patients with osteosarcoma, a cytology sample was used for diagnosis. Patients with CNS tumors were diagnosed at necropsies for being intracranial nonoperable tumors. In some of the cases, we did not have access to biopsies due to a difficult localization of tumors.

For treatment with dCelyvir, canine MSCs from healthy donors were infected with ICOCAV17 at a multiplicity of infection (MOI)

of 1 infectious particle per cell during 1 hour. Infected cells were washed 3 times, filtered, and resuspended in saline buffer. Prior to dCelyvir infusion, canine patients were treated i.v. with methylprednisone (1 mg/kg), metamizol (30 mg/kg), and difenhydramine (0.5 mg/kg). dCelyvir was administered over 45 minutes through a peripheral or central venous line (cephalic/safen preferably) at doses of 0.5×10^6 cells/kg dog body weight. During first administrations, patients were kept in the hospital for 6 hours with constant monitorization. Treatment was repeated once a week during 4 weeks. After these four administrations, the veterinary board evaluated each case and decided how to continue the treatment. Now and henceforth, when we refer to posttreatment, if not otherwise specified, we are referring to the time after the fourth dose.

During treatment, canine patients were closely followed up after dCelyvir infusions, and blood analyses were done every week in order to analyze hematologic, renal, and liver functions. Briefly, the veterinary RECIST response characterization is as follows: (i) complete response (CR): disappearance of all target lesions; pathologic LNs <10 mm short axis; (ii) PR: at least 30% reduction in the sum of diameters of target lesions, taking as a reference the baseline sum; (iii) progressive disease (PD): either the appearance of one or more new lesions or at least a 20% increase in the sum of diameters of target lesions, taking as a reference the smallest sum during the study; the sum must also show an absolute increase of 5 mm; (iv) SD: less than 30% reduction or 20% increase in the sum of diameters of target lesions, taking as a reference the smallest sum of diameters during the study. A quality of life test (18) was performed after treatment based on input from the owners.

Mouse model study

The preclinical studies in mice were approved by the "Animal Ethics Committee" of ISCIII in compliance with European Union directives. For *in vivo* imaging of dMSCs and dCelyvir homing into canine tumors, we established subcutaneous tumors in the flanks of 6- to 8-week-old NOD.CB17-Prkdc^{scid} (NOD-SCID) mice. Tumors were grown for 10 to 12 days. dMSCs or dCelyvir were incubated with 13.8 µg/mL DiR buffer for 30 minutes at 37°C according to the protocol of XenoLight DiR (Caliper Lifesciences). Then DiR-labeled dMSCs and dCelyvir were washed twice with PBS and i.p. injected in dog tumor-bearing mice (1×10^6 cells/mouse). Fluorescence imaging analysis was conducted with the IVIS 200 *in vivo* imaging system (Caliper) 24 hours after the injection. For the efficacy assays, we injected dMSCs or dCelyvir in PBS (1×10^6 cells/mouse) i.p. in the same immunodeficient model. The first dose was 5 days after tumor inoculation, and a total of three doses were administered. Tumors were measured periodically with a caliper, and volume was calculated as $(\text{length} \times \text{width}^2)\pi/6$. At day 20, mice tumors were removed and processed for flow cytometry and histology.

Cell culture

Cells were cultured in DMEM, supplemented with 10% FBS, 1% glutamine, streptomycin (100 mg/mL), and penicillin (100 U/mL), at 37°C in a humidified atmosphere with 5% CO₂. Adipose tissue from healthy dog donors was digested with collagenase IV (Sigma-Aldrich), filtered through a sterile 70 µm nylon mesh cell strainer (Fisher Scientific), and cultured in DMEM supplemented as above. Nonadherent cells were discarded through subsequent culture passages, and finally we obtained a

homogenous dMSC culture. Bone marrow-derived human MSCs were purchased from Lonza. The dMSCs/hMSC multilineage differentiation potential for adipogenic, osteogenic, and chondrogenic phenotypes was assessed by the culture of dMSCs in specific cell culture media (Cell Applications) or hMSC specific culture media (Lonza) stained with lipidic drop (oil red O), bone extracellular matrix (ECM; alizarin red), and chondrogenic glycosaminoglycans (alcian blue), respectively. DKCre cell line, a renal tumoral embryonic nonmalignant canine cell type, was a kind gift of Dr. Eric Kremer (Institut de Génétique Moléculaire, Montpellier). The Abrams canine osteosarcoma cell line was provided by Dr. David Vail (School of Veterinary Medicine, University of Wisconsin-Madison, Wisconsin). The murine non-small cell lung carcinoma cell line CMT64 was kindly gifted by Dr. Sthepan Kubicka (Hannover Medical School, Germany), and the CMT64-6 clone was selected based on its high human adenovirus replication susceptibility (19). Dog tumoral nonimmortalized cells from primary tumors were obtained after mechanical disaggregation followed by the same protocol detailed above for obtaining dMSCs. Primary cells were used after four to five passages. All cells were confirmed to be of canine origin by multispecies multiplex PCR and identified by short tandem repeat analysis. Mycoplasma infection was routinely checked by luminescence using the MycoAlert Mycoplasma Detection Kit (Lonza).

Viruses

We have previously described ICOCV17 (12). Briefly, CAV2RGD is based on CAV2, the canine wild-type virus serotype 2, with an RGD motif inserted in the HI-loop of the CAV2 fiber. ICOCV17 is a canine conditionally replicative adenovirus, based on CAV2RGD, in which the endogenous E1a promoter has been modified by inserting four palindromic E2F-binding sites, and 21 base pairs have been deleted of the E1a pRB-binding domain (E1a Δ 21) homologous to Δ 24 deletion performed in human oncolytic adenoviruses. ICOCV17 is armed with the human PH20 hyaluronidase (PH20) gene inserted after the fiber under the control of the canine IIIa protein splicing acceptor (IIIaSA).

For infectivity assays, dMSCs were seeded in 96-well plates. After 24 hours, the cells were infected in triplicate with serial dilutions of ICOCV17. After 24 hours, medium was removed, and immune staining against hexon protein was performed according to an anti-hexon staining-based method (20).

Cytotoxicity assays were performed by seeding dMSCs in 96-well plates in DMEM with 10% FBS. The cells were infected with serial dilutions of CAV2 or CAV2RGD starting with 1,000 TU/cell. Six to eight days after infection, plates were washed with PBS and stained for total protein content through absorbance measurements. For virus production, dMSCs were infected, and after 4 hours, medium was removed and cells were washed twice with PBS and incubated with fresh medium. Cells and medium (cell extract) were harvested 48 hours after infection and subjected to three rounds of freeze-thaw lysis. Viral titers of cell extracts were determined in triplicate according to an anti-hexon staining-based method in DKCre cells.

Cytokine analysis

Blood samples were collected before treatment, and serum was obtained and frozen. Analysis of GM-CSF, IFN γ , IL2, IL6, IL7, IP-10, MCP-1, and TNF α levels was performed with the

CCYTOMAG-90K, Milliplex MAP Canine Cytokine/Chemokine Magnetic Bead Panel. Other cytokines not mentioned were below the lower limits of detection.

qPCR analysis

Whole blood samples were stored at -20°C until processing. DNA was extracted from 200 μL of whole blood and was eluted with 50 μL of distilled water according to the QIAamp DNA Blood Mini Kit (Qiagen) instructions. Tumor and liver tissues were stored under different conditions; extraction of each sample was performed following different protocols. Tissue samples that were frozen at -80°C were introduced into a metal cylinder submerged in liquid nitrogen and were ground thoroughly with a pestle until they were completely pulverized. Thirty to 40 mg from each sample was used to extract DNA using the QIAamp DNA Mini Kit (Qiagen) according to the manufacturer's instructions. For samples stored at -80°C with TRIzol reagent, the tissues were thawed, vortexed during 2 minutes, and homogenized using a Potter-Elvehjem PTFE pestle with a glass tube. One mL of each sample was processed to extract DNA following the TRIzol reagent's instructions. In formalin-fixed paraffin-embedded tissues, DNA was extracted from 6 sections of 10 μm for each sample and was processed using the Cobas DNA Sample Preparation Kit (Roche) according to manufacturer's instructions. DNA quantification and purity (A260/280 and A260/230) were analyzed with Nanodrop 2000 spectrophotometer (ThermoScientific).

A standard curve was prepared based on serial dilutions of ICOCV17 from 10^8 to 10^3 vp/mL using blood from a healthy dog as diluent. DNA extraction was performed as described above for whole blood samples. Purified DNA samples were analyzed in triplicate by the quantitative real-time PCR system 7500 Fast (Applied Biosystems) using the Premix Ex Taq (Clontech), with forward primer (0.5 $\mu\text{mol/L}$) 5'-TGTGGCCTGTGTG-ATTCT-3', reverse primer (0.5 $\mu\text{mol/L}$) 5'-CCAGAATCAGCCT-CAGTGCTC-3', and 10 pmol of Taqman probe FAM-CTCGAAT-CAGTGTCAGGCTCCGCA-TAMRA, which identify E1A region. qPCR conditions were: holding stage 10 minutes at 95°C and cycling stage 15 seconds at 95°C followed by 1 minute at 60°C repeated 40 times. Analysis was performed using the 7500 Software v2.0.6 (Applied Biosystems). Positive results were confirmed by sequencing the products of the qPCR. qPCR products were treated with ExoSAP-IT (Affymetrix) following the manufacturer's instructions and were sequenced with primer at 0.6 $\mu\text{mol/L}$ using the capillary automatic sequencer DNA Analyzer 3730xl (Applied Biosystems). Sequences resulting from the sequencing process were analyzed with the basic local alignment search tool (BLAST) from the NCBI, and those that produced significant alignments were considered to be positive results.

Western blot analysis

Total protein was extracted with SDS sample buffer (62.5 mmol/L Tris, pH 6.8, 2% SDS, 10% glycerol, 1 mmol/L phenylmethylsulfonyl fluoride, 5 mmol/L NaF, 20 mmol/L β -glycerophosphate, 0.1 mmol/L Na_3VO_4 , and 1:100 protease inhibitor cocktail from Sigma). Then, samples were boiled at 95°C for 5 minutes and sonicated (three pulses of 30 seconds on ice). Protein concentrations were determined using the DC Protein Assay (Bio-Rad).

Finally, DTT and bromophenol blue were added to the samples to a final concentration of 100 mmol/L and 0.1%, respectively, and then they were boiled at 95°C for 5 minutes. Proteins were

separated by 10% SDS-PAGE and blotted onto PVDF membranes (Bio-Rad). Antibodies used are described in Supplementary Table S1. Signal was detected using the Immobilon Western chemiluminescent HRP substrate (Millipore).

Migration assays

Transwell plates (8 μm pore filters, BD Biosciences) were coated with 0.1% gelatin (Sigma), and 5×10^4 dMSCs were plated on the upper chambers. Cells were incubated in the presence of CMT64-6 or the dog tumoral cells UAX-12 or UAX-15 in the bottom chamber for 24 hours without FBS. A negative control assay was also performed by incubating the cells with only DMEM in the bottom chamber. Medium with 30% FBS was used as a positive control. Migrated cells were fixed, stained with crystal violet, and manually counted using 10 highpower fields. Experiments were repeated 3 times.

Flow cytometry

Cells were incubated with FcR blocking. For murine cells, we used mFcR blocking (Miltenyi), and for canine cells, we used hFcR Blocking (Miltenyi). We then incubated suspensions for 20 minutes at 4°C with directly conjugated antibodies diluted in PBS containing 1% FBS. For the study of cell subsets in dog peripheral blood, we dispensed 30 μL of blood per tube and lysed the erythrocytes with QuickLysis buffer (Cytognos). Tumor suspensions were obtained with mechanical disaggregation followed by enzymatic disaggregation with collagenase D at 1 mg/mL (Roche), in HBSS with Ca^{2+} and Mg^{2+} (Lonza), 2% FBS, 1 hour at 37°C. The cellular suspensions were filtered through 70 μm nylon mesh cell strainer (Fisher Scientific) and the erythrocytes lysed with QuickLysis buffer (Cytognos). The antibodies used are described in Supplementary Table S1. The analysis was conducted with a Macsquant10 flow cytometer (Miltenyi).

Immunohistochemistry

Canine biopsies were fixed in 10% formalin overnight. After that they were washed in PBS and dehydrated by immersion in graded alcohol and xylene baths. Then they were embedded in paraffin. After cooling the wax block, 5- μm -thick sections were cut in a microtome and were rehydrated (xylol, ethanol 100%, ethanol 96%, tap water) for hematoxylin-eosin staining or immunostaining. Before immunostaining, we performed antigen retrieval with citrate buffer (10 mmol/L pH 6) in a pressure cooker (2 minutes at the highest pressure). Endogenous peroxidase inhibition and blocking with normal horse serum was also performed before the overnight incubation with primary antibody at 4°C. Then after washing, the sections were incubated with biotinylated secondary antibody (RTU-Vectastain Kit) for 15 minutes, incubated with SAV-HRP during 10 minutes and after that with DAB for 3 minutes. For ICOCV17 detection, we used the polyclonal primary antibody Anti-Adenovirus 5 antibody (Abcam), followed by a secondary anti-rabbit antibody (Invitrogen). The antibodies used are described in Supplementary Table S1.

Neutralizing antibodies

To determine neutralizing antibodies (IgG) against canine adenovirus (CAV), an enzyme labeled dot assay was performed (ImmunoComb Canine VacciCheck, Biogal Galed Laboratories Acs.). Serum or whole blood samples from either pretreatment or different posttreatment time points were stored at -20°C until

analysis. Serum (5 μL) or whole blood (10 μL) samples were dispensed in the developing plate. The assay was performed at room temperature according to the manufacturer's instructions. ImmunoComb images were digitalized, and spot densities were quantified using Image Lab 5.0 Software (Bio-Rad). Arbitrary units were calculated as follows: (sample spot intensity - sample mean background intensity) - (positive reference spot intensity - positive reference spot mean background intensity).

Statistical analysis

Data were graphed and analyzed using GraphPad Prism (GraphPad Software). All experiments were performed in a blinded manner and repeated independently under identical conditions. Data distribution was examined first, and transformations were applied as appropriate. To analyze the results, the Shapiro-Wilk test was performed first to find out whether values followed a normal distribution. Then, comparisons between quantitative variables were done using the Student *t* test for samples with normal distribution, or the Wilcoxon rank-sum test (Mann-Whitney statistic), for samples with nonnormal distribution. Differences were considered significant with a *P* value below 5%. STATA software 11.0 (StataCorp) was used.

Results

dMSCs can be infected with ICOCV17 and show tumoral homing and antitumor efficacy

We treated dogs suffering from naturally occurring tumors with dCelyvir therapy consisting of dMSCs infected with a canine oncolytic virus. dMSCs were obtained from adipose tissue from healthy donors. The cells were characterized for their capability to differentiate into the three main mesodermal lineages, adipocyte, osteoblast, and chondrocyte, by studying the expression profile of MSC markers via flow cytometry (Supplementary Fig. S1A and S1B). We assessed the expression of CD90, CD29, CD73, and CD44 molecules and the absence of expression of the markers MHCII, CD3, CD11, and CD45 (Supplementary Fig. S1A). The canine oncolytic virus we used was ICOCV17, a CAV2-based, pRb-responsive, RGD-modified, and hyaluronidase-armed canine oncolytic adenovirus, which has been previously tested in dogs by direct intratumoral inoculation (12). ICOCV17 was able to infect dMSCs in a dose-dependent manner (Supplementary Fig. S1C). Compared with the wild-type virus CAV2, RGD-modified adenovirus infection resulted in higher cytotoxicity (Supplementary Fig. S1D). Production of CAVRGD in DKcre cells was consistently comparable with CAV2 productions (Supplementary Fig. S1E). Adenoviral replication in dMSCs was confirmed by immunostaining of late viral proteins (Fig. 1A) and viral protein expression quantitation by Western blot (Fig. 1B). In addition, adenoviral genome copies were quantified by qPCR at different time points after ICOCV17 infection showing a maximum production at 48 hours (Fig. 1C). In order to assess whether dMSCs or dCelyvir home into canine tumors, we performed *in vitro* transwell migration assays. Both dMSCs and dCelyvir migrated efficiently toward tumor cells (Fig. 1D).

To confirm this tropism *in vivo*, we subcutaneously inoculated canine tumors into the flanks of immunodeficient NOD-SCID mice and imaged the fluorescent signal of DiR-stained dMSCs 24 hours after i.p. administration. Fluorescent signal from the DiR-stained dMSCs was detected in the area of the tumors, and no differences between dCelyvir or dMSC delivery were found

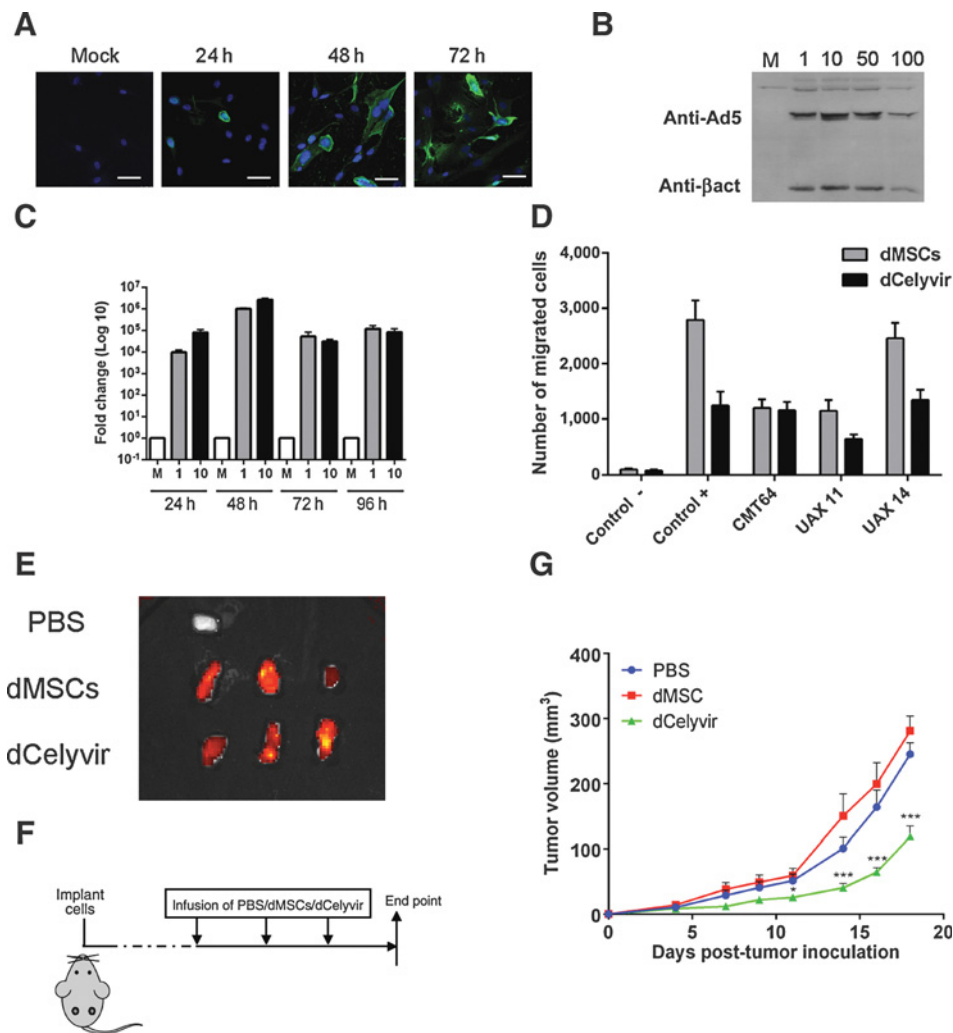


Figure 1.

Canine mesenchymal stem cells infected by canine adenoviral ICOCAV17, showing tumoral homing and antitumor efficacy in immunodeficient mice.

A, Adenovirus detection (green) in ICOCAV17-infected dMSC by immunocytochemistry. Cultures were counterstained with DAPI (blue). Representative images from three different assays performed are shown. Scale bar, 50 μ m. **B**, Western blot of adenoviral protein in dMSC at 24 hours after ICOCAV17 infection. β -Actin was measured as a loading control. **C**, Viral load was determined by qPCR in dMSC after ICOCAV17 infection (1 = MOI 1; 10 = MOI 10) and in mock-infected cells (M). The graph shows fold change (mean + SD) of two independent assays. **D**, Cell migration assays of dMSCs or dCelyvir were performed using murine tumoral CMT64-6 cell line or canine primary tumor cultures. dMSCs or dCelyvir were transferred to the upper chambers and incubated in the presence of cell culture medium (negative control), medium including FBS (positive control), CMT64-6, or primary tumor cultures in the bottom chamber for 24 hours. Migrated cells were fixed, stained with violet crystal, and counted. Bars represent the mean of triplicates + SD from three independent assays. All of them migrated significantly compared with the negative control ($P < 0.005$). **E**, Primary canine tumor cells were implanted in the flanks of NOD-SCID mice. After 15 days, DiR-stained dMSCs or DiR-stained Celyvir were i.p. infused and analyzed after 24 hours using an *in vivo* imaging system. As negative control for fluorescence, we used PBS-infused mice. Representative *ex vivo* fluorescence images of tumors are shown. **F**, Treatment schedule used in murine model. **G**, Tumor volumes in treated immunodeficient NOD-SCID mice are represented as mean + SEM.

(Fig. 1E). Overall, these results indicate that ICOCAV17 efficiently infects and replicates in dMSCs, and that these infected dMSCs (dCelyvir) reach tumors, an essential requirement for them to be used as antitumoral cellular carriers.

In order to assess the antitumoral efficacy of this approach, canine tumor-bearing NOD-SCID mice were treated with dCelyvir, dMSCs, or PBS starting 5 days after tumor inoculation with the administration of three doses (Fig. 1F). Significant differences in tumor volume between dCelyvir- and PBS-treated mice were found (Fig. 1G). Tumors treated with

dMSCs showed no differences in tumor volume compared with PBS-treated ones.

Canine patients and dCelyvir treatment

We enrolled 27 canine patients for dCelyvir therapy. The patients' clinical characteristics are shown in Table 1. The trial consisted of a repeated weekly administration of intravenous dCelyvir either alone or in combination with additional therapies according to veterinarian board choice (Table 1). A tumor biopsy was collected after the fourth dose, and a specific therapeutic

Table 1. Patients' characteristics and treatment outcome

Patients	Tumor type	Stage	P/R/Met	Diameter (cm)	Race	Gender	Age (years)	CAV vaccine	Previous lines of therapy	Therapies combination	Celyvir doses	Clinical benefit
UAX-01	Mastocytoma (low and high grade)	3A	R	5	Boxer	M	6	Y	CT	dCELYVIR	22	CR
UAX-02	Rhabdomyosarcoma	2	R	2.3	Golden retriever	M	5	Y	Mn	dCELYVIR	11	PR
UAX-03	Hemangiopericytoma	3	R	12	Siberian husky	F	15	N	Mn	dCELYVIR	3	PR
UAX-04	Osteosarcoma (osteoblastic)	ND	P	ND	Mixed	F	10	ND	CT	CT+dCELYVIR	6	SD
UAX-05	Osteosarcoma (chondroblastic)	4	P/Met	3.6	Labrador retriever	F	10	Y	CT	dCELYVIR	3	PD
UAX-06	Hemangiopericytoma	2	R	3	German shepherd	F	7	Y	-	dCELYVIR	4	PR
UAX-07	Nephroblastoma	ND	R	8.3	Labrador retriever	M	5	N	-	dCELYVIR	7	SD
UAX-08	Osteosarcoma (chondroblastic)	4	P/Met	3	Mastiff	F	12	Y	CT	CT+dCELYVIR	3	PD
UAX-09	Osteosarcoma (chondroblastic)	3	P	7.8	Leonberger	F	5	Y	-	dCELYVIR	7	PD
UAX-10	Schwannoma	3	P	5.4	Golden retriever	M	11	Y	Mn	Mn+dCELYVIR	7	PD
UAX-11	Osteosarcoma (chondroblastic)	2	P	1.3	Border Collie	F	2	N	-	dCELYVIR	4	PD
UAX-12	Hemangiopericytoma	1	P	1	Mixed	F	16	N	Mn	dCELYVIR	14	SD
UAX-13	Fibrosarcoma	1	P	7.5	Beauceron	M	10	Y	-	TKI+dCELYVIR	3	SD
UAX-14	Osteosarcoma (chondroblastic)	3	P	31	Mixed	F	8	Y	CT+TKI	TKI+dCELYVIR	6	SD
UAX-15	Mastocytoma (high grade)	ND	R	8.5	American Stafford	M	7	Y	TKI	TKI+dCELYVIR	3	PD
UAX-16	Melanoma	2	R	3	Teckel	M	13	Y	Mn+TKI	TKI+dCELYVIR	28	SD
UAX-17	Rhabdomyosarcoma	3	P	11	Labrador retriever	F	7	Y	-	dCELYVIR	13	SD
UAX-18	Fibrosarcoma	3	P	14	Mixed	M	10	Y	-	dCELYVIR	4	SD
UAX-19	Oligodendroglioma	ND	P	1	French bulldog	M	11	Y	Mn+TKI	TKI+dCELYVIR	13	SD
UAX-20	Oligodendroglioma	ND	P	1	Mixed	F	9	Y	TKI	TKI+dCELYVIR	30	CR
UAX-21	Pituitary adenoma	ND	P	3	Rottweiler	F	1	Y	-	dCELYVIR	15	SD
UAX-22	Oligodendroglioma	ND	P	1.3	French bulldog	F	8	Y	TKI	TKI+dCELYVIR	27	SD
UAX-23	Schwannoma	4	Met	7	Mixed	F	15	Y	-	dCELYVIR	10	CR
UAX-24	Hemangioma	4	Met	5.4	Greyhound	F	8	Y	CT	CT+dCELYVIR	23	CR
UAX-25	Undifferentiated pleomorphic sarcoma	3	P	3.2	French bulldog	M	5	Y	CT	dCELYVIR	11	SD
UAX-26	Hemangioma	4	Met	2.1	Greyhound	M	10	Y	CT+Mn	dCELYVIR	5	PD
UAX-27	Undifferentiated pleomorphic sarcoma	2	P	5.1	Bullmastiff	M	7	ND	CT+Mn	dCELYVIR	4	SD

Abbreviations: Stage: ND, not determined; P/R/Met, primary tumor, recurrent tumor, metastasis. The patients that presented only metastasis were cases in which primary tumors had been removed by surgery. CAV vaccine: N, nonvaccinated; ND, not determined; Y, vaccinated. Previous lines of therapy: CT, conventional chemotherapy (doxorubicin); Mn, metronomic chemotherapy (cyclophosphamide); TKI, tyrosine kinase inhibitors.

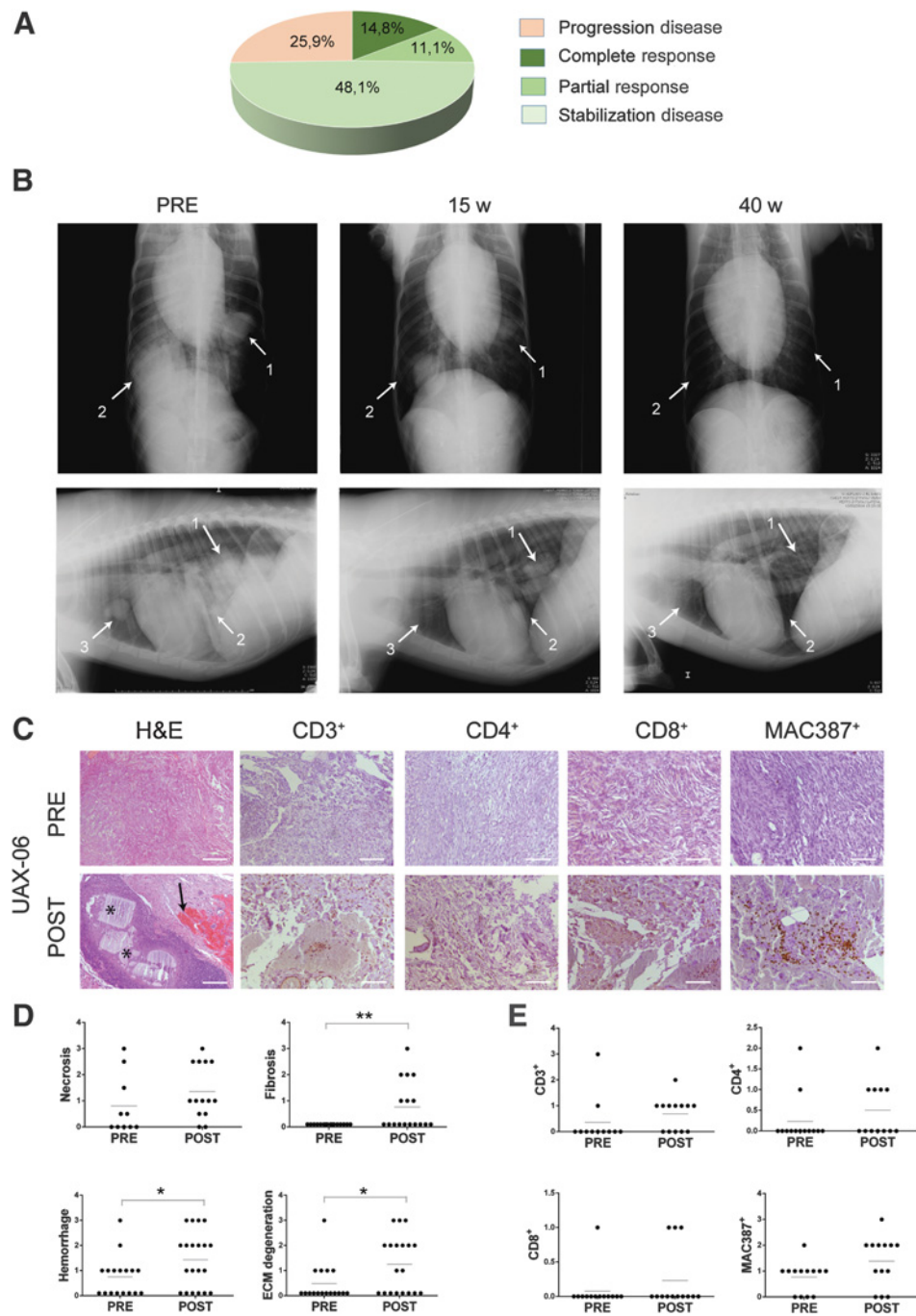


Figure 2. Clinical and anatomic-pathological results in canine patients treated with dCelyvir. **A**, Summary of clinical benefit following veterinary RECIST V1.1. **B**, X-ray images of a canine patient during dCelyvir treatment showing pulmonary metastasis evolution. Arrows, different metastatic nodules. Top images correspond to ventrodorsal views, and bottom images are lateral right views of the same dog on the same date (PRE, pretreatment; 15 w and 40 w, 15 and 40 weeks after treatment). **C**, Representative hematoxylin and eosin (H&E) staining and immunohistochemistry images from biopsies taken from tumors prior to treatment (PRE) and after the fourth dCelyvir dose (POST). Images show a representative case (UAX-06) from 20 cases analyzed. Asterisk, region with ECM degeneration; arrow, hemorrhagic area. Scale bar, 200 μ m in H&E, 100 μ m in immunohistochemistry. **D**, Graphs show semiquantitative evaluation by anatomical pathologists of structural tumor biopsies. Mean (bars) and individual values (dots) are shown. Arbitrary units were assigned by anatomical pathologists: 0, absence; 1, presence; 2, medium; and 3, abundant. Paired *t* test was performed ($n = 20$; *, $P < 0.05$; **, $P < 0.005$). **E**, Quantification of immune cells by immunohistochemistry is shown. Mean (bars) and individual values (dots) are shown.

regimen was designed for each dog based on an interim report on clinical benefit. Most dogs (59%) received dCelyvir as the only treatment, whereas the rest of the dogs were treated with combined therapies, including conventional chemotherapy in 3 dogs (three cycles of doxorubicin during 1 week plus dCelyvir for 2 weeks), tyrosine kinase inhibitors (TKI) in 7 dogs (TKIs every day plus dCelyvir once a week), or cyclophosphamide therapy in one dog (cyclophosphamide every day plus dCelyvir once a week). A group of patients with mainly suffering CNS-derived tumors and mastocytomas were also treated with corticoids (Prednisone).

Outcome assessment of dCelyvir treatment

The veterinary oncologist board evaluated the clinical responses following the four doses of dCelyvir using the veterinary RECIST V1.1 guidelines similar to human RECIST. Responses were classified as CR, PR, SD, and PD (Table 1). Seventy-four percent of the canine patients showed a clinical benefit to dCelyvir therapy with 14.8% of the cases achieving a complete remission (Fig. 2A). Twelve of 16 patients treated only with dCelyvir showed a clinical benefit (2 CR, 3 PR, and 7 SD), and 8 of 11 patients that received combined therapy showed clinical benefit (2 CR and 6 SD). Moreover, 2 of the 5 canine patients with pulmonary

Downloaded from <http://aacrjournals.org/cancerres/article-pdf/78/17/4891/28697434891.pdf> by guest on 01 February 2024

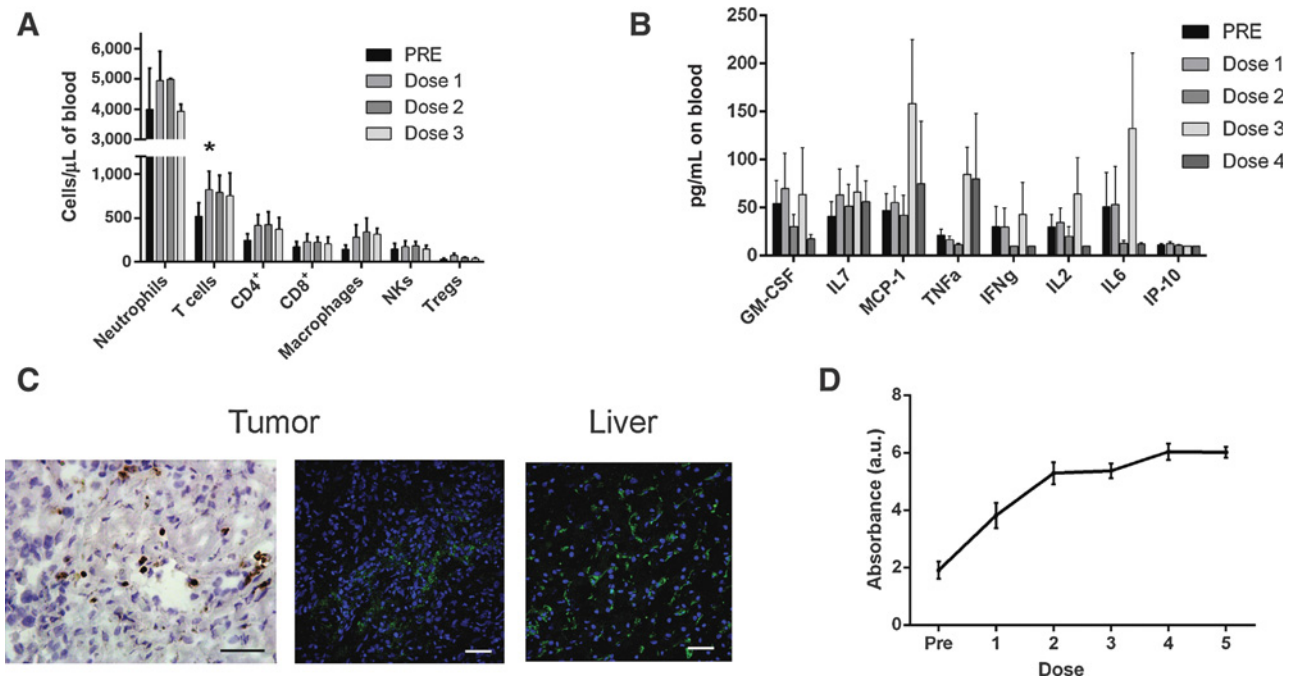


Figure 3.

Peripheral blood immune response and adenovirus detection. **A**, Total number of peripheral blood leukocytes in canine patients previous to treatment and during the first doses. Paired *t* test: *, $P < 0.05$ ($n = 15$). **B**, Cytokines in peripheral blood of canine patients are represented ($n = 10$). **C**, Representative images showing adenovirus-positive cells on FFPE biopsies (brown) and cryosections (green), including DAPI (blue) counterstaining. Scale bars, 50 μm . **D**, Antiadenoviral immunoglobulins present in serum of canine patients during dCelyvir treatment. The graph shows mean \pm SEM. All levels of antiadenoviral immunoglobulins were statistically higher compared with pretreatment values. Wilcoxon test was performed ($n = 5$ –10; $P < 0.005$).

metastasis at the time of diagnosis (UAX-05, UAX-08, UAX-23, UAX-24, and UAX-26) had a CR (Fig. 2B and Supplementary Fig. S2A). Patient UAX-24 initially received combined therapy (dCelyvir plus doxorubicin) and switched to dCelyvir only after 9 weeks, improving the clinical outcome from PR (week 15) to CR (week 40, Fig. 2B).

Anatomical pathology studies were done on tumor biopsies obtained prior to dCelyvir treatment (pretreatment, $n = 14$) and after the fourth dCelyvir dose (posttreatment, $n = 22$; Fig. 2C and Supplementary Fig. S2B). Tumor biopsies showed a significant increase in fibrosis, hemorrhages, and ECM degeneration after treatment. Necrosis evaluation showed the same tendency (Fig. 2D). Immune population analysis showed no differences of immune cell infiltration in pre- and posttreatment biopsies (Fig. 2C and E); neither when considering "responder" (CR, PR, SD) and "non-responder" (PD) groups together nor separately (Supplementary Fig. S2C). However, in posttreatment samples, we observed a trend of increased MAC387⁺ cells, including neutrophils and macrophages (Fig. 2E). Interestingly, in several cases we observed that MAC387⁺ cells were localized inside of blood vessels in pretreatment biopsies, but that they infiltrated the tumors after treatment (Supplementary Fig. S2D). Hyaluronic acid detection was performed by immunohistochemistry in pre- and posttreatment biopsies without conclusive results due to the heterogeneous patterns found within each individual sample (Supplementary Fig. S3). It should be noted that in some patients (UAX-03, UAX-09, UAX-10) during the first week after the first dose of dCelyvir, we observed an evident edema in the tumor and a transient increase in tumor volume followed by a shrinkage of

the tumor before the second dose, suggesting a temporary local tumor inflammation or pseudoprogression.

We also studied the immune cells by flow cytometry and cytokines by Multiplex \times Cytokine Panel in the peripheral blood of canine patients during the first 4 weeks (Supplementary Fig. S4A–S4D). The cell numbers of neutrophils, T cells (CD3⁺, CD4⁺, and CD8⁺), macrophages, natural killers, and Tregs tended to increase after each dose, but only an increase in T-cell numbers after the first dose was statistically significant (Fig. 3A). We did not find significant changes in cytokine levels, although we observed a slight increase in MCP-1 and IL6 following the third dose (Fig. 3B).

To measure ICOCV17 replication in tumors after dCelyvir treatment, we analyzed samples by qPCR from tumor biopsies from 12 dogs (before and after treatment), liver samples from 3 dogs (after treatment), and peripheral blood from 15 dogs (before and after treatment). All pretreatment samples and all posttreatment tumor biopsies were negative, but ICOCV17 was detected in 2 liver biopsies and 1 peripheral blood sample. The immunohistochemistry detection of ICOCV17 in tumor biopsies from 15 patients (before and after treatment) showed clusters of adenovirus-positive cells in 4 of them (Fig. 3C). Interestingly, we detected ICOCV17 in tumors despite most patients (77.7%) having been previously vaccinated against CAVs (Table 1). Measurements of anti-CAV2-neutralizing antibodies in sera indicated that these dogs had neutralizing antibodies against CAV2 prior to dCelyvir treatment. During treatment, antibody levels increased initially and tended to stabilize (Fig. 3D). It is important to highlight that high neutralizing

Table 2. Adverse events in dCelyvir-treated patients

Adverse events	Grade	
	1 and 2	3 and 4
General		
Fever	0	0
Chills	0	0
Fatigue	0	0
Myalgia	0	0
Asthenia	0	0
Sweating	0	0
Dehydration	0	0
Pain	0	0
Infection	0	0
Cachexia	0	0
Dermatologic		
Rash	1	0
Skin ulceration	0	0
Alopecia	1	0
Cardiovascular		
Hypotension	0	0
Hypertension	0	0
Hemorrhage	0	0
Gastrointestinal		
Anorexia	0	0
Dyspepsia	0	0
Nausea	0	0
Diarrhea	1	0
Vomiting	0	0
Respiratory system		
Dyspnea	0	0
Pneumonia	0	0
Apnea	0	0
Hepatic		
Liver dysfunction	0	0
Renal		
Renal dysfunction	0	0
Metabolic		
ALT increased	10	1
AST increased	1	0
Hypophosphatemia	8	0
Fibrinogen increased	0	0
Hematologic		
Leucocytes increased	0	0
Platelets decreased	0	0
Neutrophils decreased	2	0
Other		
Orchitis	1	0

NOTE: Seven of the dogs who suffered ALT increases were being treated with corticoids and three of them showed hepatic illness prior to treatment. Neutropenia was documented in two cases that were receiving concomitant treatment with doxorubicin. Events and grades have been classified following the VCOG-CTCAE v1.1.

antibody levels before and after treatment did not prevent the antitumoral effects of dCelyvir.

Safety and toxicity of dCelyvir treatment

Treatment with dCelyvir was well tolerated. We evaluated the quality of life of the canine patients, and 73% of them showed a good quality of life during the treatment (Supplementary Table S2). Most of the patients with bad quality of life presented osteosarcomas or STS that affected the legs causing restricted mobility and pain. Adverse events related to dCelyvir treatment were registered following the criteria of the veterinary cooperative oncology group for common terminology criteria of adverse events in dogs and cats (VCOG-CTCAE). Among the 27 patients, clinical adverse events were documented for only 4 of them. Two

showed skin alterations and one digestive symptoms, but these were patients that were all concomitantly treated with corticoids. Another patient suffered an orchitis (Table 2). None of these clinical adverse events were classified as severe or changed the quality of life status, and all were transient. Serum alanine transaminase (ALT) levels increased (grade 1/2) in 10 patients, but only 1 showed concomitantly high aspartate transaminase (AST) levels; an occasional decrease of phosphorus concentration was detected in eight dogs (Supplementary Fig. S5A). In addition, there were no significant changes in the peripheral blood cell counts, neither in total leukocyte number nor in hematopoietic subpopulations (Supplementary Fig. S5B). Only 2 patients showed a reduced number of neutrophils, one of which was grade 2 that subsequently recovered upon TKI removal. Of note, no significant differences between responder and nonresponder groups were observed for any of the analyzed parameters. Only a slight trend of higher ALT concentrations was observed in the responder group (Supplementary Fig. S5A). In summary, dCelyvir was a safe and well-tolerated treatment.

Discussion

Dogs with spontaneously arising cancers are an excellent model for the study of human immunotherapies and provide the opportunity to develop new veterinary oncology treatments. Oncolytic viruses represent a new class of immunotherapeutic agents that induce systemic antitumoral activity (1). In order to improve delivery of the oncolytic virus to the tumors, we used MSCs as carrier cells due to their tumor tropism. Migration of MSCs to tumors is thought to be due to inflammatory signaling in the microenvironment resembling that of an unresolved wound (21). However, the complete MSC homing mechanism remains to be elucidated (22), and tumor homing is not absolutely specific, as infused MSCs have been detected in other organs (23). Several strategies have been proposed to increase the tumor homing capability of stem cells in order for them to function as carriers (24, 25). Although theoretically an *in vivo* distribution of oncolytic virus-infected MSCs could produce a disseminated viral infection, we have not found significant toxicity using Celyvir in mice (19), dogs (this article), or humans (7, 26). Also, we have never detected adenoviral genomes in peripheral blood, except at a peak of 72 hours after the first dCelyvir infusion. Both observations indicate effective immune-neutralizing activity in peripheral organs. In this regard, almost all treated dogs were previously vaccinated with a CAV-2-based vaccine and showed high levels of neutralizing antibodies, which increased quickly after dCelyvir administration until reaching a plateau. This is in agreement with the antibody kinetics shown in human patients infused with other oncolytic viruses (27–29). However, these high antibody levels did not preclude achieving a high rate of clinical benefit (74%), including 14.8% achieving CRs that were maintained for years.

Although different types of tumors were included in the study, most of them were STS. Surgery remains the main treatment for STS due to its biological behavior and its poor response to chemotherapy and radiotherapy. Recurrence following surgical resection is the main reason for treatment failure (30–32). This is probably due to small buds of sarcoma cells regularly extruding through the reactive zone to form small isolated nodules (satellite nodules or skip metastases; refs. 32, 33). Tumor recurrence is 10 times more likely in dogs with incomplete margins with a

recurrence rate of 17% to 28% (34, 35). In our study, we obtained a longer disease-free survival time suggestive of an antitumoral adaptative immune activation, which is supported by the lymphocyte infiltration observed in the tumor samples analyzed. A trend of increased CD3⁺ cell infiltration was seen in nonresponders compared with responders (Supplementary Fig. S2C). We observed similar effects in the context of the compassionate use of Celyvir in humans. In contrast to responders, nonresponder patients showed increased peripheral blood cell counts and increases in the proportions of terminally differentiated effector T lymphocytes during Celyvir treatment (7). These results may be indicative of an antiadenoviral response. Viral antigens usually contain immunodominant epitopes that elicit strong antiviral immune responses, which may limit the development of robust antitumor immunity (36). Therefore, we hypothesize that a less active antiadenoviral response in responder patients allows them to develop a better antitumor response. Moreover, cellular vehicles can serve to evade antiviral mechanisms encountered in the bloodstream, prevent uptake by off-target tissues, and favor their homing to tumor beds where they can produce thousands of oncolytic viruses. After adenoviral secretion and tumor infection, an immune response would be activated involving the activation of immunostimulatory genes, including those implicated in chemotaxis, inflammation, T-cell regulation, and antigen presentation. This infiltration of immune cells might favorably change the immunosuppressive status of the tumor microenvironment and increase cell infiltration. In the present study, we also observed that the number of CD3⁺ and MAC387⁺ cells in the patients' tumor biopsies tended to increase with the treatment.

ICOCV17 expresses hyaluronidase, an enzyme that hydrolyzes hyaluronan, a primary macromolecular component of the ECM of solid malignancies. This enzyme has antitumoral properties as a single agent. Hyaluronidase inhibited tumor growth in xenograft models, and it has been used in early clinical trials (37). However, a recent phase II clinical trial (NCT01839487) testing hyaluronidase in combination with chemotherapy was transiently halted because of associated toxicity. In our approach, dCelyvir should restrict hyaluronidase expression to tumor sites and, consequently, limit systemic side effects. It is probably responsible for the increased ECM disaggregation we observed in posttreatment tumor biopsies, thereby enhancing virus spread and immune cell infiltration throughout the tumor. However, our data on this respect are not conclusive.

tion throughout the tumor. However, our data on this respect are not conclusive.

In summary, dCelyvir has shown clinical efficacy with very low toxicity. dCelyvir has also shown the capacity to transform the tumor microenvironment toward more susceptibility to immune activation. This could benefit it as a candidate for combination therapy with immune checkpoint inhibitors.

Disclosure of Potential Conflicts of Interest

No potential conflicts of interest were disclosed.

Authors' Contributions

Conception and design: T. Cejalvo, E. Laborda, J. Garcia-Castro
Development of methodology: T. Cejalvo, A.J. Peris-Barrios, I. del Portillo, E. Laborda, I. Cubillo, F. Vázquez, M. Ramirez, J. Garcia-Castro
Acquisition of data (provided animals, acquired and managed patients, provided facilities, etc.): T. Cejalvo, A.J. Peris-Barrios, I. del Portillo, E. Laborda, M.A. Rodriguez-Milla, I. Cubillo, F. Vázquez, D. Sardón, N. del Castillo
Analysis and interpretation of data (e.g., statistical analysis, biostatistics, computational analysis): T. Cejalvo, A.J. Peris-Barrios, D. Sardón, M. Ramirez, R. Alemany, J. Garcia-Castro
Writing, review, and/or revision of the manuscript: T. Cejalvo, A.J. Peris-Barrios, E. Laborda, M.A. Rodriguez-Milla, D. Sardón, M. Ramirez, R. Alemany, N. del Castillo, J. Garcia-Castro
Administrative, technical, or material support (i.e., reporting or organizing data, constructing databases): M.A. Rodriguez-Milla, F. Vázquez
Study supervision: F. Vázquez, J. Garcia-Castro
Other (administration of the treatment): I. del Portillo

Acknowledgments

We want to thank the staff of Veterinary Hospital, the technical staff from the Anatomic-pathological Department, as well as Carolina Jiménez and Giulia Setti for their participation in our studies. We are grateful to A. Gómez Vitores for useful advice on the pathology studies. J. Garcia-Castro was awarded grants from the Fondo de Investigaciones Sanitarias (FIS: PI11/00377, PI17CIII/00013, RD12/0036/0027), the Madrid Regional Government (CellCAM; P2010/BMD-2420), and the Asociación Pablo Ugarte (G86121019). The experiments were approved by the appropriate committees.

The costs of publication of this article were defrayed in part by the payment of page charges. This article must therefore be hereby marked *advertisement* in accordance with 18 U.S.C. Section 1734 solely to indicate this fact.

Received December 4, 2017; revised April 17, 2018; accepted July 5, 2018; published first July 10, 2018.

References

- Kaufman HL, Kohlhapp FJ, Zloza A. Oncolytic viruses: a new class of immunotherapy drugs. *Nat Rev Drug Discov* 2015;14:642–62.
- Ferguson MS, Lemoine NR, Wang Y. Systemic delivery of oncolytic viruses: hopes and hurdles. *Adv Virol* 2012;2012:805629.
- Power AT, Bell JC. Taming the Trojan horse: optimizing dynamic carrier cell/oncolytic virus systems for cancer biotherapy. *Gene Ther* 2008;15:772–9.
- Ramirez M, Garcia-Castro J, Alemany R. Oncolytic virotherapy for neuroblastoma. *Discov Med* 2010;10:387–93.
- Cascallo M, Alonso MM, Rojas JJ, Perez-Gimenez A, Fueyo J, Alemany R. Systemic toxicity-efficacy profile of ICOVIR-5, a potent and selective oncolytic adenovirus based on the pRB pathway. *Mol Ther* 2007;15:1607–15.
- Garcia-Castro J, Alemany R, Cascallo M, Martinez-Quintanilla J, Arriero Mdel M, Lassaletta A, et al. Treatment of metastatic neuroblastoma with systemic oncolytic virotherapy delivered by autologous mesenchymal stem cells: an exploratory study. *Cancer Gene Ther* 2010;17:476–83.
- Melen GJ, Franco-Luzon L, Ruano D, Gonzalez-Murillo A, Alfranca A, Casco F, et al. Influence of carrier cells on the clinical outcome of children with neuroblastoma treated with high dose of oncolytic adenovirus delivered in mesenchymal stem cells. *Cancer Lett* 2016;371:161–70.
- Paoloni M, Khanna C. Translation of new cancer treatments from pet dogs to humans. *Nat Rev Cancer* 2008;8:147–56.
- Kol A, Arzi B, Athanasiou KA, Farmer DL, Nolte JA, Rebhun RB, et al. Companion animals: translational scientist's new best friends. *Sci Transl Med* 2015;7:308ps21.
- Alvarez CE. Naturally occurring cancers in dogs: insights for translational genetics and medicine. *ILAR J* 2014;55:16–45.
- Khanna C, Lindblad-Toh K, Vail D, London C, Bergman P, Barber L, et al. The dog as a cancer model. *Nat Biotechnol* 2006;24:1065–6.
- Laborda E, Puig-Saus C, Rodriguez-Garcia A, Moreno R, Cascallo M, Pastor J, et al. A pRb-responsive, RGD-modified, and hyaluronidase-armed canine oncolytic adenovirus for application in veterinary oncology. *Mol Ther* 2014;22:986–98.

13. Linch M, Miah AB, Thway K, Judson IR, Benson C. Systemic treatment of soft-tissue sarcoma-gold standard and novel therapies. *Nat Rev Clin Oncol* 2014;11:187–202.
14. Clark MA, Fisher C, Judson I, Thomas JM. Soft-tissue sarcomas in adults. *N Engl J Med* 2005;353:701–11.
15. Tseng WW, Somaiah N, Engleman EG. Potential for immunotherapy in soft tissue sarcoma. *Hum Vaccin Immunother* 2014;10:3117–24.
16. Lettieri CK, Hingorani P, Kolb EA. Progress of oncolytic viruses in sarcomas. *Expert Rev Anticancer Ther* 2012;12:229–42.
17. Liikanen I, Ahtiainen L, Hirvonen ML, Bramante S, Cerullo V, Nokisalmi P, et al. Oncolytic adenovirus with temozolomide induces autophagy and antitumor immune responses in cancer patients. *Mol Ther* 2013;21:1212–23.
18. Villalobos AE. Quality-of-life assessment techniques for veterinarians. *Vet Clin North Am Small Anim Pract* 2011;41:519–29.
19. Rincon E, Cejalvo T, Kanojia D, Alfranca A, Rodriguez-Milla MA, Hoyos RAG, et al. Mesenchymal stem cell carriers enhance antitumor efficacy of oncolytic adenoviruses in an immunocompetent mouse model. *Oncotarget* 2017;8:45415–31.
20. Alcayaga-Miranda F, Cascallo M, Rojas JJ, Pastor J, Alemany R. Osteosarcoma cells as carriers to allow antitumor activity of canine oncolytic adenovirus in the presence of neutralizing antibodies. *Cancer Gene Ther* 2010;17:792–802.
21. Spaeth E, Klopp A, Dembinski J, Andreeff M, Marini F. Inflammation and tumor microenvironments: defining the migratory itinerary of mesenchymal stem cells. *Gene Ther* 2008;15:730–8.
22. Karp JM, Leng Teo GS. Mesenchymal stem cell homing: the devil is in the details. *Cell Stem Cell* 2009;4:206–16.
23. Nakashima H, Kaur B, Chiocca EA. Directing systemic oncolytic viral delivery to tumors via carrier cells. *Cytokine Growth Factor Rev* 2010;21:119–26.
24. Stuckey DW, Shah K. Stem cell-based therapies for cancer treatment: separating hope from hype. *Nat Rev Cancer* 2014;14:683–91.
25. Kang SK, Shin IS, Ko MS, Jo JY, Ra JC. Journey of mesenchymal stem cells for homing: strategies to enhance efficacy and safety of stem cell therapy. *Stem Cells Int* 2012;2012:342968.
26. Rubio R, Garcia-Castro J, Gutierrez-Aranda I, Paramio J, Santos M, Catalina P, et al. Deficiency in p53 but not retinoblastoma induces the transformation of mesenchymal stem cells in vitro and initiates leiomyosarcoma in vivo. *Cancer Research* 2010;70:4185–94.
27. Laurie SA, Bell JC, Atkins HL, Roach J, Bamat MK, O'Neil JD, et al. A phase 1 clinical study of intravenous administration of PV701, an oncolytic virus, using two-step desensitization. *Clin Cancer Res* 2006;12:2555–62.
28. Hwang TH, Moon A, Burke J, Ribas A, Stephenson J, Breitbart CJ, et al. A mechanistic proof-of-concept clinical trial with JX-594, a targeted multi-mechanistic oncolytic poxvirus, in patients with metastatic melanoma. *Mol Ther* 2011;19:1913–22.
29. Koski A, Raki M, Nokisalmi P, Liikanen I, Kangasniemi L, Joensuu T, et al. Verapamil results in increased blood levels of oncolytic adenovirus in treatment of patients with advanced cancer. *Mol Ther* 2012;20:221–9.
30. Ehrhart N. Soft-tissue sarcomas in dogs: a review. *J Am Anim Hosp Assoc* 2005;41:241–6.
31. Liptak J. The future for surgical margins. *J Small Anim Pract* 2013;54:563.
32. Kind M, Stock N, Coindre JM. Histology and imaging of soft tissue sarcomas. *Eur J Radiol* 2009;72:6–15.
33. Enneking WF, Spanier SS, Malawer MM. The effect of the anatomic setting on the results of surgical procedures for soft parts sarcoma of the thigh. *Cancer* 1981;47:1005–22.
34. Kuntz CA, Dermell WS, Powers BE, Devitt C, Straw RC, Withrow SJ. Prognostic factors for surgical treatment of soft-tissue sarcomas in dogs: 75 cases (1986–1996). *J Am Vet Med Assoc* 1997;211:1147–51.
35. McSporrán KD. Histologic grade predicts recurrence for marginally excised canine subcutaneous soft tissue sarcomas. *Vet Pathol* 2009;46:928–33.
36. Yewdell JW. Confronting complexity: real-world immunodominance in antiviral CD8+ T cell responses. *Immunity* 2006;25:533–43.
37. Hingorani SR, Harris WP, Beck JT, Berdov BA, Wagner SA, Pshevlotsky EM, et al. Phase Ib Study of PEGylated recombinant human hyaluronidase and gemcitabine in patients with advanced pancreatic cancer. *Clin Cancer Res* 2016;22:2848–54.